Journal of Applied Electrochemistry (2005) 35:837–843
DOI 10.1007/s10800-005-1322-7

Correlation between accelerated corrosion tests and atmospheric corrosion tests on steel

CHUEN-CHANG LIN* and CHI-XIANG WANG
Department of Chemical Engineering, National Yunlin University of Science and Technology, 123 University Road, Sec. 3, Yunlin, Taiwan, R.O.C.
*(*author for correspondence, e-mail: linchuen@pine.yuntech.edu.tw, tel.: +886-5-534-2601, fax: +886-5-534-2601)*

Received 13 April 2004; accepted in revised form 23 December 2004

Key words: accelerated corrosion, atmospheric corrosion, sodium chloride, steel

Abstract

Three kinds of steel [soft steel (SPHC), carbon steel (SS400), and weathered steel (A588)] were prepared for accelerated corrosion and atmospheric corrosion tests. The results of atmospheric corrosion tests were similar to those of accelerated corrosion tests. A correlation was developed for prediction of atmospheric corrosion rates of steel using atmospheric corrosion factors (i.e. Cl^- deposition fluxes, time of wetness, and temperatures). The comparisons between predicted and measured thickness losses due to atmospheric corrosion showed an average error of 31.6%. In addition, Tafel plots were employed to evaluate the corrosion behaviour of the three kinds of steel. The morphology of the cross-sections of specimens exposed outdoors was examined by scanning electron microscopy (SEM). The results of the Tafel extrapolation tests and SEM observations of the surface morphology were similar to those seen in the atmospheric corrosion tests.

1. Introduction

Atmospheric corrosion rates of steel in subtropical regions can reach the most serious classes (C_4 and C_5) according to ISO 9223 [1]. Thus, in order to build steel atmospheric corrosion databases, outdoor exposure tests are necessary. However, these take considerable expense and time (from several months to several years). To reduce the outdoor atmospheric corrosion test time, laboratory accelerated corrosion tests were utilized to investigate the correlation between corrosion factors and corrosion rates. Finally, the aim was to predict steel atmospheric corrosion rates based on corrosion factors (i.e. Cl^- deposition fluxes, time of wetness, and temperatures) in the real environment.

2. Research methods

The object of this study was to establish the correlation between corrosion rates and corrosion factors. Thus it was necessary to carry out laboratory accelerated corrosion tests under various corrosion factors. The current work focused on Cl^- deposition fluxes, time of wetness, and temperatures in a salt chamber and a constant temperature/humidity (RH = 60%) chamber. In addition, the study included atmospheric corrosion tests whose corrosion rates were compared with corrosion rates predicted by the correlation. The three kinds of test specimens (SS400, SPHC, and A588) were provided by China Steel Company and their chemical compositions are listed in Table 1. In according with the ASTM G50-76 standard [2], the size of test specimens for atmospheric corrosion tests was $150 \times 100 \times 2$ mm^3, whereas the size of test specimens for accelerated corrosion tests was $150 \times 50 \times 2$ mm^3 . Before the test, each specimen was abraded with coarse (mesh #100) SiC papers, and then with fine (mesh #600) SiC papers, then rinsed ultrasonically with distilled water and acetone for 3 min. It was then rinsed with distilled water alone, dried, and weighed to four decimals.

Atmospheric corrosion tests were carried out at a station on the roof of a four-story building, open to the air and 2500–3000 m away from the seashore. The pretreated test specimens (SPHC, SS400, and A588) were exposed to the atmosphere on open racks at an angle of 45° facing south. After different exposure duration determined by corrosion rates (the higher the corrosion rate, the shorter the exposure period), test specimens were immersed in 50% (volume/volume) aqueous HCl containing a corrosion inhibitor $[(CH_2)_6N_4]$[3] until the complete elimination of corrosion products was achieved according to the ISO 8407 standard [4]. They were then rinsed with distilled water, dried, and weighed to four decimals, so that weight losses due to atmospheric corrosion could be obtained. Atmospheric corrosion

Table 1. Chemical compositions (wt.%) of test specimens

Element type	C	Si	Mn	P	S	Cu	Cr	Ni	V	Al
SPHC	0.03	0.02	0.28	0.014	0.009	0.01	0.02	0.01	–	0.042
SS400	0.13	0.02	0.77	0.021	0.007	0.01	0.02	0.01	0.002	0.032
A588	0.15	0.25	1.50	0.022	0.015	0.28	0.44	0.18	0.035	–

rates in coastal regions are mainly dependent on Cl^- deposition fluxes, temperatures, metal species, and time of wetness. Cl^- deposition fluxes were measured by the wet candle method according to ISO 9225 [5] at the same station of atmospheric corrosion tests and at different periods (Table 2) determined by exposure duration (Table 3) of tests on the steel. The wet candle method consists of the deployment of a dry cotton fabric of known areas exposed under a shed. The amount of Cl^- deposited on the gauge was determined analytically at the end of the exposure period and then the Cl^- deposition flux calculated.

Due to the real environment conditions being variable, it was difficult to isolate the correlation between corrosion rates and corrosion factors by atmospheric corrosion tests alone. In order to better understand the correlation between corrosion rates and corrosion factors, accelerated corrosion tests in the laboratory were utilized to model atmospheric corrosion. The chosen variables for the accelerated corrosion tests were different temperatures (288, 298, and 308 K) and Cl^- deposition fluxes (0 mg Cl^- day^{-1} m^{-2}, 100 mg Cl^- day^{-1} m^{-2}, and 2500 mg Cl^- day^{-1} m^{-2}). The choice without Cl^- deposition flux (0 mg Cl^- day^{-1} m^{-2}) in the corrosion tests was to find the active energy of corrosion without Cl^- and frequency factors of the corrosion rate constant. The choice of the Cl^- deposition fluxes (100 mg Cl^- day^{-1} m^{-2} and 2500 mg Cl^- day^{-1} m^{-2}) in the corrosion tests was to accelerate corrosion rates. In accordance with the ASTM B117-97 standard, the test specimens were put in the salt chamber and were faced to the sprayer at an angle of 30°. Salt concentrations were varied to model different Cl^- deposition fluxes and temperatures were varied according to a range of temperatures measured in the meteorological station near the atmospheric corrosion station. In order to accurately model outdoor cyclic dry–wet conditions, the test specimens were exposed to the salt chamber (wet condition) for 4 h in each dry–wet cycle (24 h for one dry–wet cycle), followed by placing them in the constant temperature/humidity chamber (dry condition) for 20 h in each cycle. The ratio of wet to dry conditions was chosen to model local climate records of rainy days to fine days. After accelerated corrosion tests, test specimens were treated to eliminate the corrosion products according to the ISO 8407 standard [4]. Finally, the correlation between corrosion rates and corrosion factors could be determined utilizing the data from accelerated corrosion tests.

Table 2. Cl^- deposition fluxes of different periods

Periods	[Cl^-]/mg Cl^- day^{-1} m^{-2}
2001/8/24 to 2001/9/26	39.57
2001/9/27 to 2001/10/26	98.47
2001/10/27 to 2001/12/3	94.41
2001/12/4 to 2002/1/7	75.37
2002/1/8 to 2002/2/28	56.75
2002/3/1 to 2002/6/5	33.43
2001/6/6 to 2002/8/14	40.23

Table 3. Atmospheric corrosion factors

Exposure duration	T/K	t_w/year	[Cl^-]/g Cl^- $year^{-1}$ m^{-2}
2001/8/24 to 2001/9/26	301.7	0.063	14.44
2001/8/24 to 2001/10/26	300.3	0.120	24.68
2001/8/24 to 2001/12/3	298.2	0.150	28.36
2001/8/24 to 2002/1/7	296.9	0.192	28.14
2001/8/24 to 2002/2/28	295.3	0.250	26.09
2001/8/24 to 2002/6/5	296.2	0.390	21.15
2001/8/24 to 2002/8/14	301.5	0.480	24.42

Tafel plots were obtained through an EG&G M352 corrosion measurement system. The electrolyte, a solution of 0.1 M NaCl and 0.1 M Na_2SO_4, was prepared from reagent grade chemicals and distilled water. A three-electrode corrosion cell consisted of Ag/AgCl as the reference electrode, Pt as the counter electrode and the test specimens (SPHC, SS400, and A588) cleaned of corrosion products as the working electrode. All the corrosion experiments were conducted at room temperature and the potentials reported are against the Ag/AgCl reference electrode except where stated. In addition, examination of the surface morphology of the cross-sections of specimens exposed to outdoor conditions was conducted by SEM (HITACHI S3000N, Japan) in the range 20–25 keV.

3. Results and discussion

Corvo et a1. [6], Mendoza and Corvo [7], and Morcillo [8] found that Cl^- deposition fluxes were dependent on wind directions, wind speeds, precipitation, the distances from the seashore, and other factors. Cl^- deposition fluxes measured by the wet candle method for different periods at the atmospheric corrosion station are shown in Table 2. All the Cl^- deposition fluxes were below 100 mgCl^- day^{-1} m^{-2} due to the sampling station being 2500–3000 m away from the seashore. They were higher during fall and winter because of higher wind speed and lower precipitation but were lower during summer due to lower wind speed and higher precipitation.

The results of atmospheric corrosion tests for the three test specimens are illustrated in Figure 1. The weight loss for SPHC was higher than that of both A588 and SS400. The weight loss for A588 was similar to that for SS400 during the initial 150 days, because corrosion products on A588 were still not dense enough to protect the specimens. However, after 150 days, the curve for A588 began to plateau. In contrast, the corrosion rates (slopes of Figure 1) for SS400 and SPHC only began to

decrease after 200 days. The reason behind this behaviour may be the greater wt.% of other elements in sample A588 (Table 1) and that protective layers of corrosion built up more quickly on A588 than either SS400 or SPHC. Furthermore, the gradual formation of corrosion layers was almost certainly responsible for the decrease in corrosion rates on all samples with increasing time.

Weight losses as a function of time for the three kinds of steel at different temperatures but without Cl^- deposition flux in the salt chamber are illustrated in Figures 2–4, which reveal that the higher the temperature, the higher the corrosion rate (slopes of Figures 2–4). This is in agreement with Arrhenius' law and the positive active energy (Table 4) of corrosion. In addition, Figures 2–4 also show that the weight loss for A588 was less than that of SS400 and SPHC at the same temperature and near the plateau region. Once again, this picture may be the result of greater wt.% of other elements in sample A588. Weight losses as a function of time for the three kinds of steel after exposure to the different Cl^- deposition fluxes (100 mg Cl^- day^{-1} m^{-2} and 2500 mg Cl^- day^{-1} m^{-2}) and temperatures (298 and 308 K) in the environment chambers are illustrated in Figures 5–7. They show that for the same temperature, higher Cl^- deposition fluxes lead to higher corrosion rates (slopes of Figures 5 and 7), because Cl^- acts as a catalyst to reduce active energy of corrosion and inhibits protective layers forming on test specimens. For the same Cl^- deposition flux, higher temperatures result in higher corrosion rates (slopes of Figures 6 and 7). Once again, the weight loss of A588 was less than that of SS400 and SPHC near the plateau region. Furthermore, the tendencies of corrosive characteristic for the three kinds of steel were similar to those seen in the atmospheric corrosion tests (Figure 1).

According to previous literature [9–12], the corrosion rates for steel in coastal areas were mainly dependent on the Cl^- deposition fluxes, time of wetness, steel species, and temperatures. Therefore, the following correlation

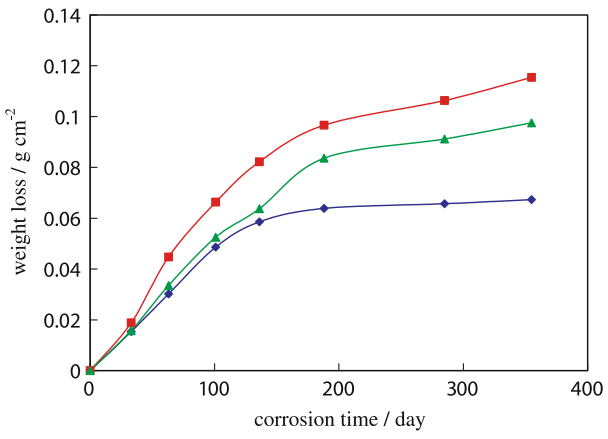

Fig. 1. Weight losses as a function of corrosion time for the three kinds of steel in the atmospheric corrosion station (■: SPHC, ▲: SS400, ◆: A588).

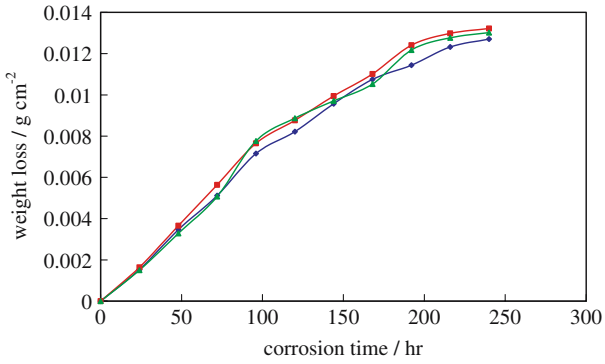

Fig. 2. Weight losses as a function of corrosion time for the three kinds of steel at T = 288 K in the salt chamber (RH = 99%, ■: SPHC, ▲: SS400, ◆: A588).

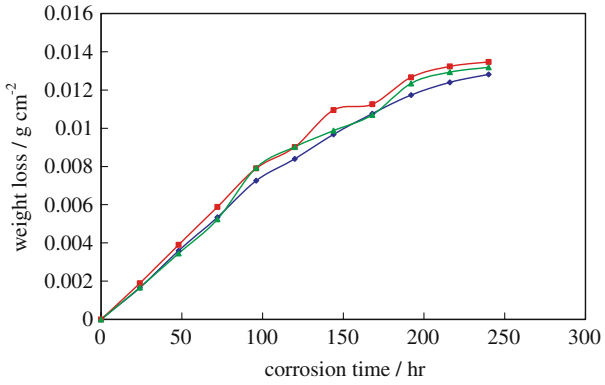

Fig. 3. Weight losses as a function of corrosion time for the three kinds of steel at T = 298 K in the salt chamber (RH = 99%, ■: SPHC, ▲: SS400, ◆: A588).

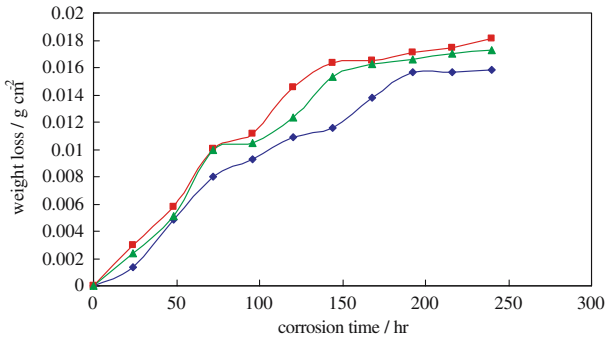

Fig. 4. Weight losses as a function of corrosion time for the three kinds of steel at T = 308 K in the salt chamber (RH = 99%, ■: SPHC, ▲: SS400, ◆: A588).

(Equation 1) between corrosion rates and corrosion factors was deduced from corrosion theory and Arrhenius' law, which could be used to predict atmospheric corrosion rates. The active energy of corrosion without Cl^- and frequency factors of the corrosion rate constant for the three kinds of steel could be found from Equation 1 utilizing the experimental data (slopes of $Corr/t_w$ and temperatures shown in Figures 2–4). First, Equation 1 was expressed as natural logarithms. Then

Table 4. Parameters of Equation 1 for test specimens

Type	A/μm year^{-1}	E°/cal mol^{-1}	a_1	a_2
SPHC	46166.05	2476.4	18.172	−0.0203
SS400	37873.24	2367.1	19.432	−0.0217
A588	67608.30	2784.6	17.813	−0.0198

the values of $E°$ and A could be calculated from the slope $[-E°/(RT)]$ and intercept (ln A) of a plot of In (Corr/t_w) vs. $1/T$. The results are listed in Table 4. Furthermore, the regression coefficients (a_1 and a_2) for the three kinds of steel could also be found by expressing Equation 1 as natural logarithms and entering the values for $E°$, A, and the experimental data (slopes of Corr/t_w, temperatures, and Cl^- deposition fluxes shown in Figures 5–7). Values of a_1 and a_2 could then be solved from three simultaneous equations. The results are also listed in Table 4.

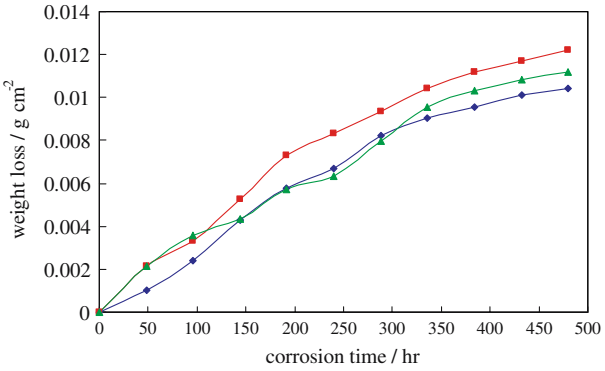

Fig. 5. Weight losses as a function of corrosion time for the three kinds of steel in the salt chamber and then in the constant temperature/humidity chamber (Cl^- deposition flux = 100 mg Cl^- day^{-1} m^{-2}, dry time/wet time = 5/1, 24 h for one dry–wet cycle, T = 308 K, ■: SPHC, ▲: SS400, ◆: A588).

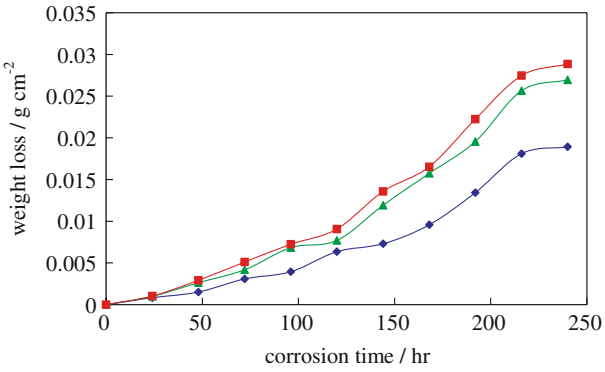

Fig. 6. Weight losses as a function of corrosion time for the three kinds of steel in the salt chamber and then in the constant temperature/humidity chamber (Cl^- deposition flux = 2500 mg Cl^- day^{-1} m^{-2}, dry time/wet time = 5/1, 24 h for one dry–wet cycle, T = 298 K, ■: SPHC, ▲: SS400, ◆: A588).

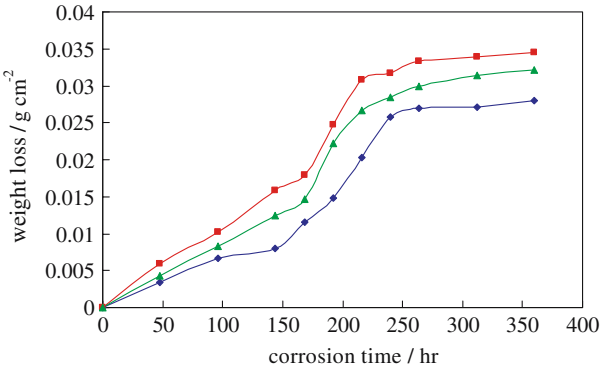

Fig. 7. Weight losses as a function of corrosion time for the three kinds of steel in the salt chamber and then in the constant temperature/humidity chamber (Cl^- deposition flux = 2500 mg Cl^- day^{-1} m^{-2}, dry time/wet time = 5/1, 24 h for one dry–wet cycle, T = 308 K, ■: SPHC, ▲: SS400, ◆: A588).

$$\mathrm{Corr}/t_w = A\mathrm{e}^{-E/(RT)} \quad (1)$$

where Corr is the thickness loss (μm) which is converted from the weight loss divided by the iron density (7.86 g cm^{-3}) due to smaller wt.% of the other elements except iron (see Table 1), t_w is the time of wetness (year) – the corrosion duration during which the relative humidity (RH) is in excess of 80% and the temperature is above 0 °C, A is the frequency factor (μm year^{-1}) of the corrosion rate constant, E is the active energy (cal mol^{-1}) of corrosion with Cl^- deposition flux ($E = E° + a_1[Cl^-] + a_2[Cl^-]^2$, Cl^- acts as a catalyst to reduce active energy of corrosion and inhibits protective layers forming on test specimens [9]), $E°$ is the active energy (cal mol^{-1}) of corrosion without Cl^-, a_1 and a_2 are the regression coefficients, $[Cl^-]$ is the Cl^- deposition flux (g Cl^- year^{-1} m^{-2}), R is the gas constant (1.987 cal mol^{-1} K^{-1}), and T is the temperature (K).

Thus thickness losses due to atmospheric corrosion could be predicted by Equation 1 utilizing atmospheric corrosion factors (Table 3) whose time of wetness can be determined from RH/temperature measured in the meteorological station and Cl^- deposition fluxes were obtained from Table 2. The comparisons between predicted and measured thickness losses due to atmospheric corrosion showed errors of SPHC: 29.01%, SS400: 28.67%, and A588: 37.18% (see Figures 8–10). The linear regression analyses for thickness losses between prediction and measurement due to atmospheric corrosion showed good fits (SPHC: R^2 = 0.78, SS400: R^2 = 0.80, and A588: R^2 = 0.65). However, the slopes of the regression analysis line are greater than one, so the model simulation results are underestimations due to reduction of oxygen diffusion through the corrosion overburden and other atmospheric corrosion factors (SO_2, etc.) not being considered in Equation 1.

Corrosion data obtained from Tafel curves (Figure 11) [13] are I_{corr} = 7.56 × 10^{-8} A cm^{-2} (E_{corr} = −0.18 V) for

A588, $I_{corr} = 1.916 \times 10^{-7}$ A cm^{-2} ($E_{corr} = -0.224$ V) for SS400, and $I_{corr} = 4.634 \times 10^{-7}$ A cm^{-2} ($E_{corr} = -0.38$ V) for SPHC. The corrosion current density of A588 was the lowest and that of SPHC was the highest. Therefore, A588 had the best anticorrosion due to the lowest corrosion current density and SPHC had the worst anticorrosion due to the highest corrosion current density. For tendencies of anticorrosive characteristic, the results of Tafel extrapolation tests were similar to those seen in the atmospheric corrosion tests (Figure 1).

Red brown rust appeared on the surface after the steel had been exposed to the atmospheric environment and rust compactness can affect corrosion rates. For outdoor exposure tests, rust dots appeared on the surface of the steel in the initial stages, and then rust spread across the entire surface. After a several-month exposure, rust bubbles appeared on the surface and parts of rust were striped from the steel. At the end of the exposure period, cross-sections were prepared for SEM evaluation, Figures 12 and 13, show SEM images of SPHC and SS400 after 6 months exposure outdoors, and illustrate much corrosion pitting due to exposure to the Cl^- environment and formation of less compact rust. In contrast, Figure 14 shows an SEM image of A588 after 6 months outdoor exposure, showing less corrosion pitting. Thus the SEM results confirm the weight loss data shown in Figure 1.

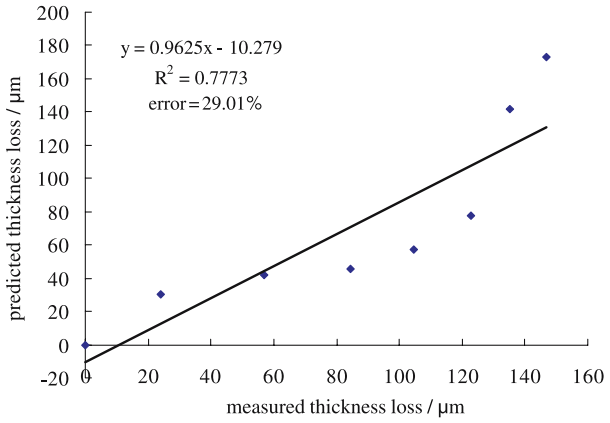

Fig. 8. Comparison between predicted and measured thickness loss for atmospheric corrosion of SPHC.

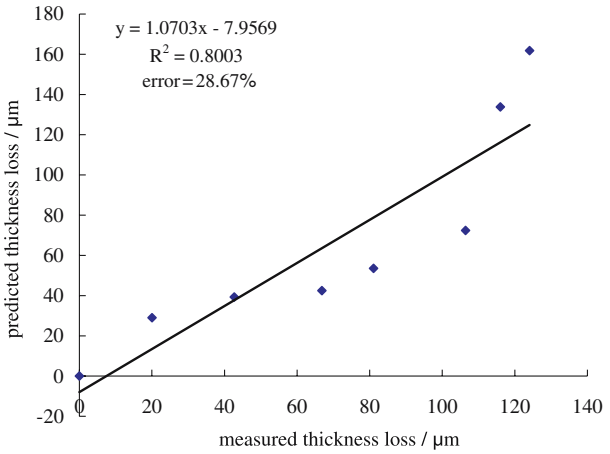

Fig. 9. Comparison between predicted and measured thickness loss for atmospheric corrosion of SS400.

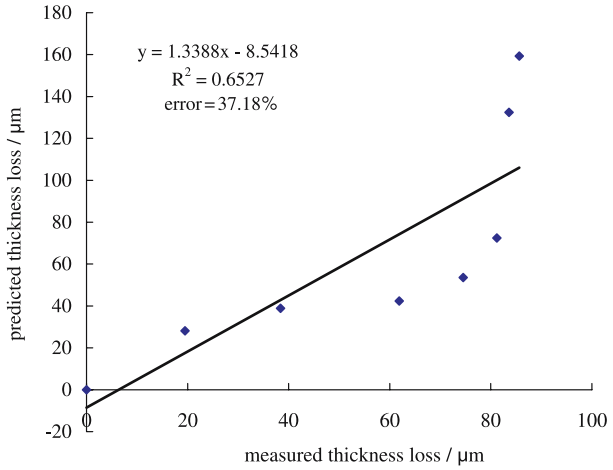

Fig. 10. Comparison between predicted and measured thickness loss for atmospheric corrosion of A588.

4. Conclusions

The results of accelerated corrosion test indicated that the higher the Cl^- deposition flux, the higher the corrosion rate. The results of atmospheric corrosion tests illustrate that the weight loss for SPHC was higher than that for SS400 which was, in turn, higher than A588. A similar pattern was seen in the accelerated corrosion tests. In addition, the comparisons between predicted and measured thickness losses due to atmospheric corrosion showed errors of SPHC: 29.01%, SS400: 28.67%, and A588:37.18%.

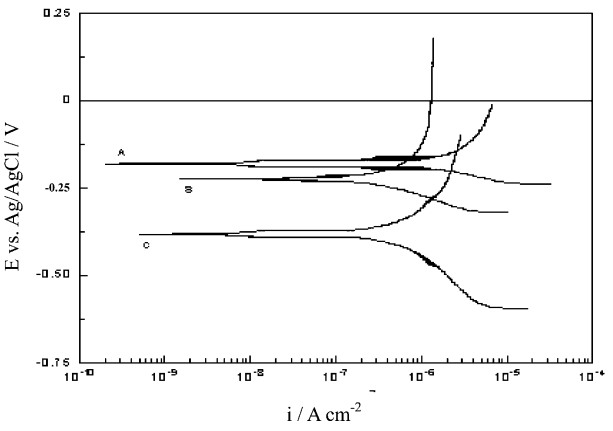

Fig. 11. Tafel curves of the three kinds of steel in the aqueous solution (0.1 M NaCl and 0.1 M Na_2SO_4) (A: A588, S: SS400, C: SPHC).

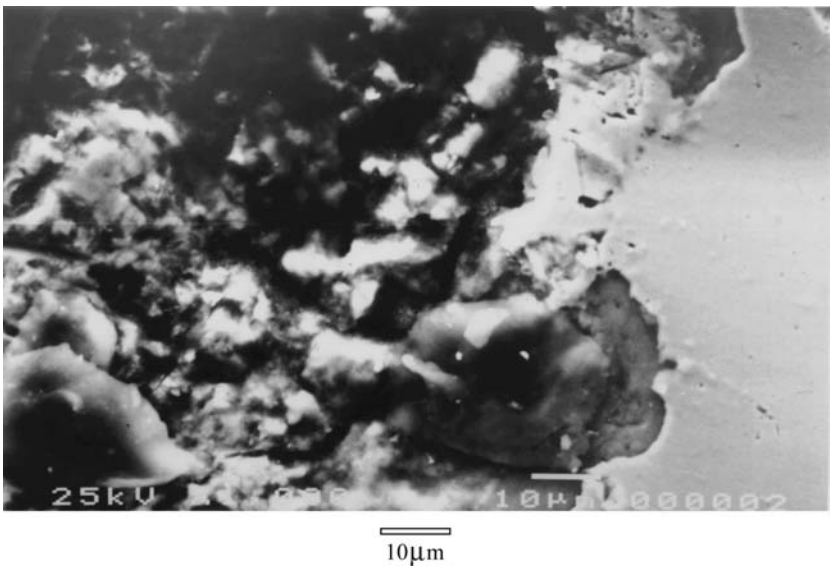

Fig. 12. SEM photograph of a cross-section of SPHC after 6 months outdoor exposure.

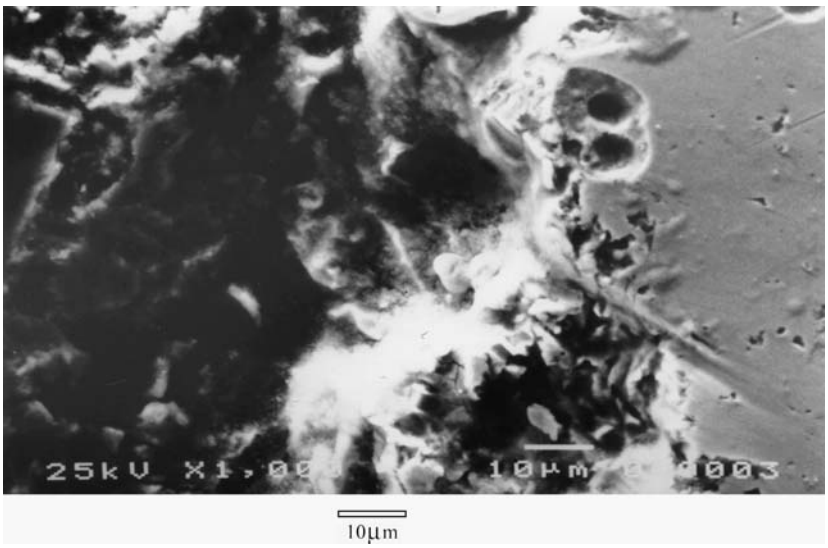

Fig. 13. SEM photograph of a cross-section of SS400 after 6 months outdoor exposure.

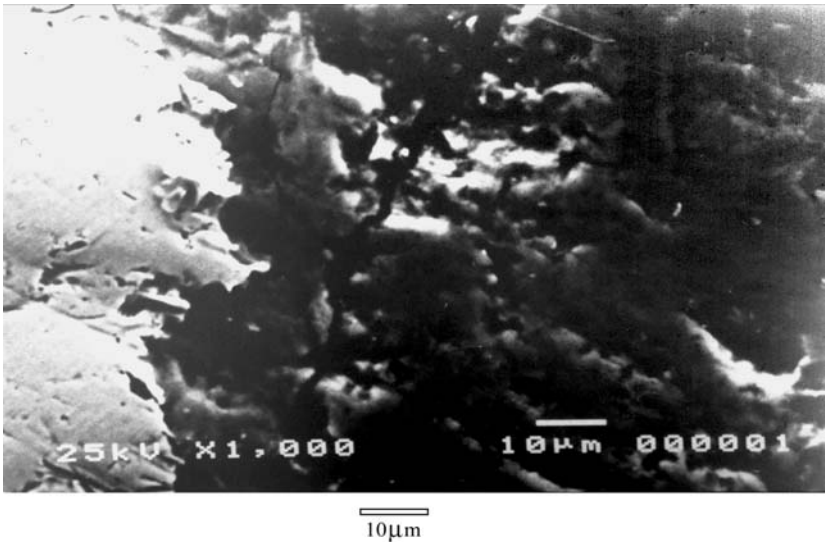

Fig. 14. SEM photograph of a cross-section of A588 after 6 months outdoor exposure.

Acknowledgements

Financial support by the National Science Council of the Republic of China (under Grant no. NSC 90-2214-E-224-010) is gratefully acknowledged.

References

1. ISO 9223, 'Corrosion of Metal and Alloys – Classification of Corrosivity of Atmospheres'.
2. ASTM G50-76, 'Standard Recommended Practice for Conducting Atmospheric Corrosion Tests on Metals'.
3. A. Philip and P.E. Schweitzer, 'Corrosion and Corrosion Protection Handbook', 2nd ed. (Marcel Dekker Inc., Atmospheric Corrosion Tests on Metals, Annual Book of ASTM Standards, 1988).
4. ISO 8407, 'Corrosion of Metal and Alloys – Removal of Corrosion Products from Corrosion Test Specimens'.
5. ISO 9225, 'Corrosion of Metal and Alloys – Corrosivity of Atmospheres – Methods of Measurement of Pollution'.
6. F. Corvo, C. Haces, N. Betancourt, L. Maldonado, L. Veleva, M. Echeverria, O.T. De Rincon and A. Rincon, *Corrosion Sci.* **39** (1997) 823.
7. A.R. Mendoza and F. Corvo, *Corrosion Sci.* **41** (1999) 75.
8. M. Morcillo, *Corrosion Sci.* **42** (2000) 91.
9. R.P. Vera Cruz, A. Nishikata and T. Tsura, *Corrosion Sci.* **40** (1998) 125.
10. R. Ericsson, *Werkstoffe und Korrosion* **29** (1978) 400.
11. S. Oesch, *Corrosion Sci.* **38** (1996) 1357.
12. P.J. Sereda, *Corrosion in Natural Environments* (ASTM Spec. Tech. Publ., Philadelphia, 1974), pp. 558.
13. S.W. Dean, in R. Baboian (ed.), 'Electrochemical Technique for Corrosion Engineering', (NACE, 1986).